White-light Fourier transformer with low chromatic aberration

Pedro Andrés, Jesús Lancis, and Walter D. Furlan

A simple Fourier transformation system working with broadband parallel illumination is presented. The proposed setup, consisting of two on-axis zone plates and an achromatic objective, allows us to obtain the achromatic Fourier transform representation of the input at a finite distance with a low chromatic aberration. The discussion of the system, using the Fresnel diffraction theory, leads to an analytical expression to evaluate the transversal and longitudinal chromatic aberrations. It is shown that the resulting chromatic aberrations for typical values of the involved parameters are less than 1% over the entire visible spectrum.

Key words: Achromatic Fourier transform, incoherent processing.

1. Introduction

In the frame of optical information processing, two different kinds of optical processors—those working under spatially incoherent but monochromatic illumination and those working under spatially coherent but temporally incoherent illumination—are becoming more frequently used. Partially coherent systems are characterized by their multichannel nature. Thus they are suitable for processing information in a parallel way, and consequently for improving the signal-to-noise ratio.[1,2]

The treatment of a system under polychromatic point-source illumination can be extended to the coherent case if each wavelength acts as an independent channel to which coherent processing is applied. Therefore, the diffraction pattern results as the incoherent superposition of the different monochromatic patterns. Nevertheless, because of the wavelength dependence of the diffraction phenomenon, a broadband spectral-bandwidth illumination introduces a new drawback in Fourier processors. This drawback is the chromatic blurring of the Fourier transform representation.

P. Andres and W. D. Furlan are with the Departamento de Optica, Universidad de Valencia, 46100 Burjasot, Spain; J. Lancis is with the Departamento Ciencias Experimentales, Universitat Jaume I, 12080 Castellón, Spain. W. D. Furlan is on leave from the Comisión de Investigaciones Cientificas, Centro de Investigaciones Opticas, Buenos Aires, Argentina.

Received June 19, 1991.
0003-6935/92/234682-06$05.00/0.

Achromatic processors are designed to compensate for the chromatic dispersion introduced by the broadband illumination, making the achromatization of the whole Fraunhofer diffraction pattern of the input simultaneously. The optical Fourier transform of an ideal achromatic transformer is located in a single Fraunhofer plane with the same magnification for each wavelength.[3]

Several methods to produce an achromatic Fourier transformation have been reported. Most of the proposed setups use specially designed dispersive lenses. Some of them employ all-glass elements,[4] and others use a combination of holographic optical elements with appropriate dispersive objectives.[5,6] Moreover, certain easily implemented achromatic Fourier transform systems have also been proposed.[7–9] These systems are composed of two zone plates and two nondispersive lenses. The latter devices permit the development of some applications in optical matched filtering and other optical processing techniques that use polychromatic illumination. A special mention must be made of Katyl's study,[10] in which he proposed an achromatic setup composed of a zone plate and a closely separated doublet, which was made of a cemented achromat and a second zone plate.

In this paper we develop a first-order theory for obtaining a novel white-light achromatic Fourier transformer. The system is composed of only two on-axis zone plates and an achromat objective. Our proposal allows us to obtain the achromatic Fourier transform (AFT) at finite distances with low chromatic aberrations. In a certain way Katyl also developed a first-order theory, but our approach, which

leads to a different arrangement, allows us to obtain a simple relationship for the residual chromatic aberration and then a criterion is given in order to minimize it. In Section 2, we briefly discuss the image-formation properties of a kinoform zone plate using geometric optics considerations. In Section 3 we describe the achromatic Fourier transformation system. In Section 4, the proposed system is analyzed in the context of the paraxial Fresnel diffraction theory. Finally, in Section 5, the residual lateral and longitudinal chromatic aberrations are calculated. Some examples for typical values of the involved parameters of the system are shown.

2. Imaging Properties of Kinoform Zone Plates Under Polychromatic Illumination

To present the basic features of our achromatic Fourier transformer, we rewrite the properties of image formation of a blazed zone plate as follows.

First we consider an on-axis kinoform zone plate ZP_1, with an image focal length $Z'(\sigma) = Z_0'\sigma/\sigma_0$ (where the constant Z_0' represents the focal distance for the wave number σ_0) placed at a distance d_1 from a plane object O normal to the optical axis of the system [see Fig. 1(a)]. Because of wave-number dependence of the focal distance of ZP_1, each wavelength of the incident light generates an image with a different axial position and transverse magnification. Using the Gaussian lens formula,

$$(1/d_1) + (1/d_1') = 1/Z', \tag{1}$$

we find that the images of O illuminated by polychromatic light are located at distances

$$d_1'(\sigma) = d_1 Z_0'\sigma/(d_1\sigma_0 - Z_0'\sigma). \tag{2}$$

Throughout the study all distances are directed, with the sign convention that those in the same sense as the entering light are positive (in our case from left to right) and vice versa. In Fig. 1(a) O and O'(σ) are shown as real planes (d_1 and d_1' are positive distances), but in general they can lie anywhere in their proper optical spaces.

The size and orientation of each image produced by the thin zone plate can be simply determined by using the undeviated ray through the optical center of ZP_1 [see Fig. 1(a)]. Therefore, using a broad-spectrum light, we find that the set of images dispersed along the optical axis constitutes the frustum of right cone V.

Conversely, a set of chromatic plane objects that form a frustum of the cone is imaged by a zone plate ZP_2 of focal length $-Z'(\sigma)$ in a single, and then achromatic, image at an arbitrary distance d_2' [see Fig. 1(b)] when the two following conditions are fulfilled: (1) the optical center of ZP_2 coincides with the point from which all the objects subtend the same angle and (2) taking into account Eqs. (1) and (2), we find that the distances to ZP_2 from the objects are

$$d_2(\sigma) = -d_2'Z_0'\sigma/(d_2'\sigma_0 + Z_0'\sigma). \tag{3}$$

Consequently, the objects must be axially dispersed according to the expression

$$\dot{d}_2(\sigma) = -d_2'^2 Z_0'\sigma_0/(d_2'\sigma_0 + Z_0'\sigma)^2, \tag{4}$$

where $\dot{x} = dx/d\sigma$.

The above results find practical applications in the optical implementation of an AFT at finite distances, as we show in Section 3.

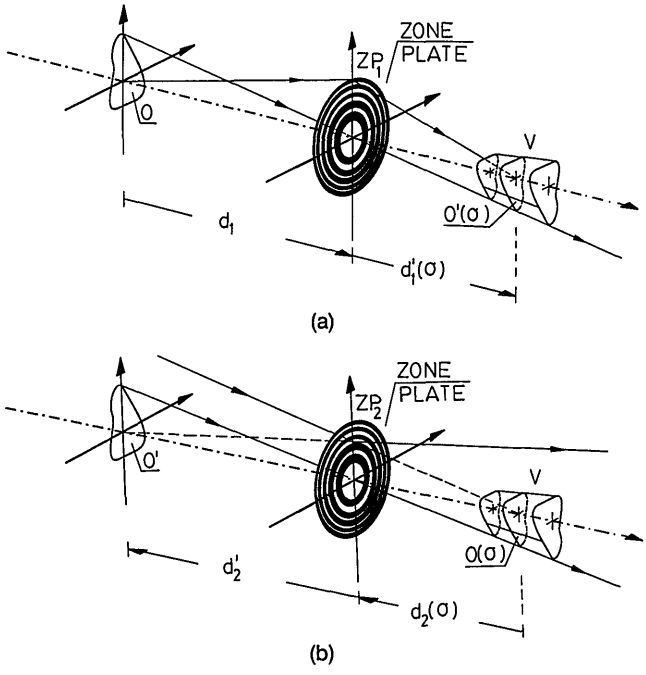

Fig. 1. Imaging properties of a zone plate using broad-spectrum light: (a) the chromatic images of O formed by ZP_1 are displayed in a volume V; and (b) the chromatic objects O(σ) forming V can be imaged through a zone plane ZP_2 in a single achromatic image O'.

3. Achromatic Fourier Transformation

The optical setup of revolution for obtaining the AFT is depicted in Fig. 2. The input transparency is illuminated with a white-light collimated beam. The kinoform zone plate ZP_1 provides the Fraunhofer diffraction pattern of the input signal for each spectral component of the incident light at its corresponding image focal plane, i.e., at a normal distance $Z(\sigma) = Z_0\sigma/\sigma_0$. In this way an arbitrary spatial frequency (u, v) of the object is located at different planes for every wavelength, but with the same transversal magnification, i.e., $x = Z_0u/\sigma_0$ and $y = Z_0v/\sigma_0$. Hence the same spatial frequency lies along a straight line parallel to the optical axis. Moreover, for a broad-spectrum illumination the set of spatial frequencies with the same modulus $\rho = \sqrt{u^2 + v^2}$ generates a cylindrical surface defining a volume V'.

The achromatic objective L placed at a distance l from ZP_1 images V' into a frustum of the right circular cone V'' (see Fig. 2). The apex of the cone coincides with the image focal point of L. It is straightforward to show that the distances to this

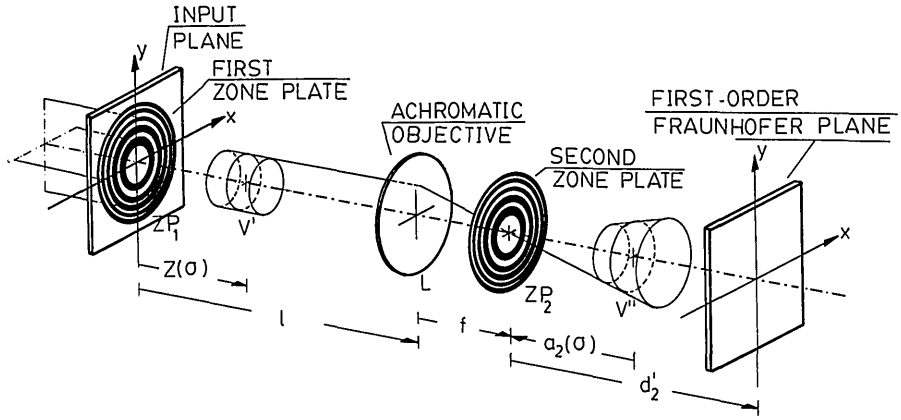

Fig. 2. Setup for the achromatic Fourier transformer. The symbols used in the text are also shown. Note that the volume V'' lies in the object space of ZP_2.

point from the chromatic Fraunhofer patterns forming the volume V'' are given by

$$a_2(\sigma) = -f^2\sigma_0/[\sigma_0(l - 0f) - Z_0\sigma], \tag{5}$$

where f is the focal length of the objective L. Therefore, the chromatic dispersion of the above images along the optical axis is

$$\dot{a}_2(\sigma) = -f^2Z_0\sigma_0/[\sigma_0(l - f) - Z_0\sigma]^2. \tag{6}$$

Taking into account the results in Section 2, we see that, if the diffraction patterns constituting V'' are dispersed in the same manner as those in volume V in Fig. 1(b), a second zone plate ZP_2, placed at the image focal plane of L (something that implies that $f > 0$) will compress such volume into a single image, thereby providing the AFT of the input. Therefore, to achieve an exact agreement between V and V'', we set

$$a_2(\sigma) = d_2(\sigma). \tag{7}$$

Nevertheless, by comparing Eqs. (3) and (5) we see that there are no set of values for f, l, Z_0, d_2', and Z_0' that fulfill the above condition, because the functional dependence of d_2 and a_2 on σ are qualitatively different.

Alternatively, because the range of wave numbers corresponding to the visible spectrum is narrow—in this study we consider the interval between $\sigma_1 = 1.4$ μm^{-1} and $\sigma_2 = 2.5$ μm^{-1}—we develop a first-order theory. We expand both functions $a_2(\sigma)$ and $d_2(\sigma)$ as a Taylor series at a point σ_0 ($\sigma_1 < \sigma_0 < \sigma_2$) and we replace Eq. (7) by the less restrictive conditions

$$a_2(\sigma_0) = d_2(\sigma_0), \qquad \dot{a}_2(\sigma_0) = \dot{d}_2(\sigma_0). \tag{8}$$

By substituting Eqs. (3), (4), (5), and (6) into Eq. (8), with $\sigma = \sigma_0$, we obtain

$$f^2/(l - f - Z_0) = d_2'Z_0'/(d_2' + Z_0'),$$
$$f^2Z_0/(l - f - Z_0)^2 = d_2'^2Z_0'/(d_2' + Z_0')^2.$$

The above equation system can be solved for the unknown quantities Z_0' and l, with Z_0, f, and d_2' as parameters. The results are

$$Z_0' = f^2/Z_0, \tag{9}$$

$$l = 2Z_0 + f + (f^2/d_2'). \tag{10}$$

Consequently, to obtain the AFT of the input at a distance d_2' from ZP_2, we must ensure that the achromat L is located at a distance l from ZP_1, given by Eq. (10); the focal length of ZP_2 must be $Z'(\sigma) = -Z_0'\sigma/\sigma_0 = -f^2\sigma/Z_0\sigma_0$. We have already stated that f is a positive number, but the parameter d_2' must also be greater than zero in order to obtain a real AFT. Nevertheless, the parameter Z_0 is permitted to be positive or negative, provided the value of l remains positive. In both cases the focal-length sign of ZP_2 always is opposite that of ZP_1.

Because higher-order terms are not considered in the expansions of $a_2(\sigma)$ and $d_2(\sigma)$, the proposed setup will suffer from residual chromatic aberration. To evaluate the chromatic abberation, in Section 4 we obtain the location and the scale of the optical Fourier transform for every spectral component of the light by using the paraxial Fresnel diffraction theory.

4. Theoretical Analysis

Let an input transparency with amplitude transmittance $t(x, y)$ be uniformly illuminated by a normally incident, white-light plane wave. For simplicity, the input is assumed to be placed against the first zone plate ZP_1. Thus, the amplitude distribution just behind ZP_1 for any spectral component is

$$U_0(x, y) = t(x, y)\exp[-i\pi\sigma_0(x^2 + y^2)/Z_0]. \tag{11}$$

Assuming the Fresnel approximations to be valid for the propagation over the distances l and f and taking into account the phase effects of both the lens L and the zone plate ZP_2 (see Fig. 2), we find the field amplitude leaving ZP_2 for the wave number σ to be

$$U_1(x, y) = \exp\{i\pi\sigma(x^2 + y^2)[(1/f) - (l/f^2) - \sigma_0/\sigma Z_0')]\}$$
$$\times \iint_{-\infty}^{\infty} t(x', y')\exp[-i\pi\sigma_0(x'^2 + y'^2)/Z_0]$$
$$\times \exp[-i2\pi\sigma(xx' + yy')/f]dx'dy'. \tag{12}$$

Finally, with Eqs. (9) and (10) satisfied and by using the Fresnel diffraction formula once again, we can write the complex amplitude at a distance d_2' from ZP_2 as

$$U_2(x,y) = \exp[i\pi\sigma(x^2+y^2)/B] \iint_{-\infty}^{\infty} t(x',y') \times \exp[i\pi(x'^2+y'^2)(\sigma-\sigma_0)^2/Z_0(2\sigma-\sigma_0)] \times \exp[-i2\pi A(xx'+yy')]dx'dy', \quad (13)$$

where

$$A = f\sigma^2/[d_2'Z_0(\sigma_0-2\sigma)], \quad (14)$$

and B, the distance from the paraxial image plane to this reference plane, is given by

$$B = d_2'/[1 - f^2\sigma/d_2'Z_0(\sigma_0-2\sigma)]. \quad (15)$$

Inspection of Eq. (13) reveals that the Fourier transform representation of $t(x, y)$ is obtained, aside from the multiplicative quadratic phase factor preceding the integral, at the first-order Fraunhofer plane only for $\sigma = \sigma_0$. The scale of the above Fourier transformation is

$$x = -Z_0d_2'u/\sigma_0f, \qquad y = -Z_0d_2'v/\sigma_0f. \quad (16)$$

For $\sigma \neq \sigma_0$ the integral of Eq. (13) does not become a Fourier transform. Now the function U_2 can be thought of as an out-of-focus image of the Fraunhofer diffraction pattern of the input signal. In fact, in the vicinity of the preceding plane, at a distance $R' = d_2' + R$ from ZP_2 the field amplitude for the wave number σ can be written as

$$U_3(x,y) = \exp[i\pi\sigma(x^2+y^2)/(B+R)] \times \iint_{-\infty}^{\infty} t(x'\sigma/BA, y'\sigma/BA)\exp[i\pi(\sigma-\sigma_0)^2\sigma^2 \times (x'^2+y'^2)/Z_0(2\sigma-\sigma_0)B^2A^2] \times \exp[i2\pi\sigma W_{20}(x'^2+y'^2)] \times \exp[i2\pi\sigma(xx'+yy')/(B+R)]dx'dy', \quad (17)$$

where W_{20} denotes the defocus coefficient of the aberration function, which with the present notation takes the form $W_{20} = -R/2B(B+R)$. If the product of the two quadratic phase terms with x'^2 and y'^2 is unity, the integral again describes the Fourier transform of the input signal. This condition is satisfied for distances $R'(\sigma)$ given by

$$R'(\sigma) = \{(1/d_2') - [Z_0(\sigma-\sigma_0)^2/f^2\sigma\sigma_0]\}^{-1}. \quad (18)$$

Therefore, for each wave number the in-focus Fraunhofer pattern is generally achieved in a different longitudinal position, and consequently the scale of the transform must be evaluated in the corresponding transverse plane. From Eqs. (17) and (18), we find that the scaling of the Fourier transform is

$$x(\sigma) = -Z_0fd_2'\sigma u/[f^2\sigma\sigma_0 - Z_0d_2'(\sigma-\sigma_0)^2],$$
$$y(\sigma) = -Z_0fd_2'\sigma v/[f^2\sigma\sigma_0 - Z_0d_2'(\sigma-\sigma_0)^2]. \quad (19)$$

Of course, for $\sigma = \sigma_0$ Eq. (18) becomes $R'(\sigma_0) = d_2'$ and Eq. (19) leads to the former Eq. (16).

Note that a quadratic phase factor, which is different for each wave number, precedes the transform integral in Eq. (17). In the present study we do not take into account the above phase curvature since we are interested in an AFT in intensity.

Because the location of the Fraunhofer plane and the scale of the transform are σ dependent, the setup exhibits an intrinsic residual chromatic aberration, both longitudinal and transversal, that is evaluated in the next section.

5. Paraxial Residual Chromatic Aberrations

The fractional difference between the axial position of the Fraunhofer pattern for the wave number σ and for the wave number σ_0 for which achromatism was effected is a good indication of the magnitude of the paraxial residual longitudinal chromatic aberration, LCA_0, of the suggested system. In mathematical terms, the above quantity expressed as percentage is given by

$$LCA_0(\sigma;\sigma_0) = 100[R'(\sigma) - d_2']/d_2'. \quad (20)$$

Similarly, for the paraxial transversal chromatic aberration, TCA_0, we have

$$TCA_0(\sigma;\sigma_0) = 100[x(\sigma) - x(\sigma_0)]/x(\sigma_0) = 100[y(\sigma) - y(\sigma_0)]/y(\sigma_0). \quad (21)$$

The substitution of Eqs. (18) and (19) into Eqs. (20) and (21), respectively, gives

$$LCA_0(\sigma;\sigma_0) = TCA_0(\sigma;\sigma_0) = 100\{[f^2\sigma\sigma_0/Z_0d_2'(\sigma-\sigma_0)^2] - 1\}^{-1}. \quad (22)$$

Note the interesting fact that both chromatic errors have an identical expression. Hereafter we will refer to either of them as the chromatic aberration, $CA_0(\sigma;\sigma_0)$, of the system. Besides, if $\alpha = f^2/Z_0d_2'$ is positive (a fact which implies $Z_0 > 0$), generally CA_0 is a nonnegative function; i.e., $R'(\sigma) \geq d_2'$ and $x(\sigma) \geq x(\sigma_0)$ for every σ corresponding to the visible region of the electromagnetic spectrum. The graphical interpretation of these statements is shown in Fig. 3. In contrast, $\alpha < 0$ implies $CA_0 \leq$ for all σ.

The chromatic aberration $CA_0(\sigma;\sigma_0)$ is dependent only on the choice of the parameter σ_0 and the value of the quantity α. The optical transformer will have a smaller chromatic aberration for a greater value of $|\alpha|$, with a fixed σ_0. Moreover, the variation of CA_0

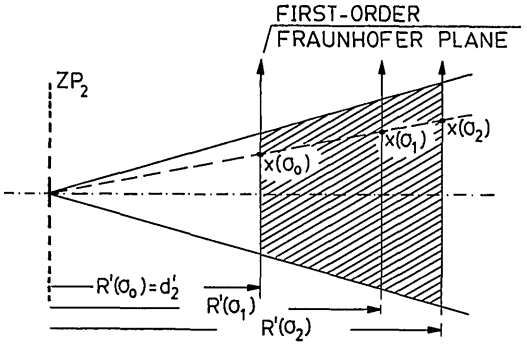

Fig. 3. Scale and axial position of the Fourier transform vary with σ in such a way that an arbitrary frequency always subtends the same angle from the optical center of ZP_2. The hatched region represents the image of the volume V'' in Fig. 2 through ZP_2 when a conventional but positive value of α is assumed.

versus σ over the visible spectrum is rather different depending on the selected value of σ_0, as is shown in Fig. 4. For a fixed value of α, the chromatic error remains as small as possible over the whole interval $[\sigma_1, \sigma_2]$ when the function CA_0 takes the same value at the end wave numbers. The mathematical equation

$$CA_0(\sigma_1; \sigma_0) = CA_0(\sigma_2; \sigma_0) \tag{23}$$

has the solution, from Eq. (22), of

$$\sigma_0 = \sqrt{\sigma_1\sigma_2}, \tag{24}$$

or equivalently $\lambda_0 = \sqrt{\lambda_1\lambda_2}$. For instance, if $\sigma_1 = 1.4$ μm^{-1} and $\sigma_2 = 2.5$ μm^{-1}, Eq. (24) provides $\sigma_0 = 1.87$ μm^{-1}. The dashed curve in Fig. 4 corresponds to this value of σ_0. The relative axial position and lateral magnification of the Fraunhofer patterns, when $\sigma_0 = \sqrt{\sigma_1\sigma_2}$, are shown in Fig. 5. Here, by combining Eq. (23) with Eqs. (20) and (21), we get $R'(\sigma_1) = R'(\sigma_2)$ and $x(\sigma_1) = x(\sigma_2)$, respectively. Thus, the Fraunhofer patterns for σ_1 and σ_2 coalesce.

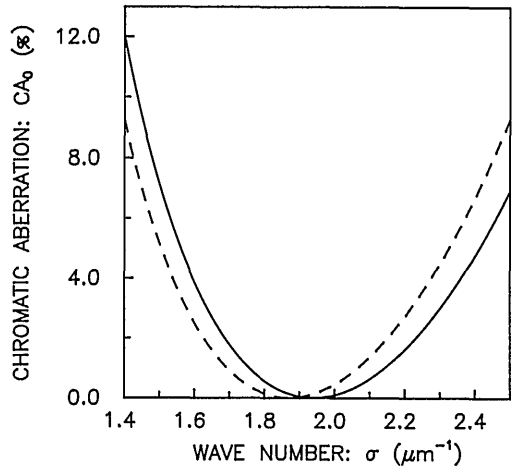

Fig. 4. Residual chromatic aberration of the system design in Fig. 2 for $\alpha = 1$ (e.g., $f = d_2' = Z_0 = 300$ mm) and with the following values for the parameter σ_0: solid curve, $\sigma_0 = 1.94$ μm^{-1}; dashed curve, $\sigma_0 = 1.87$ μm^{-1}.

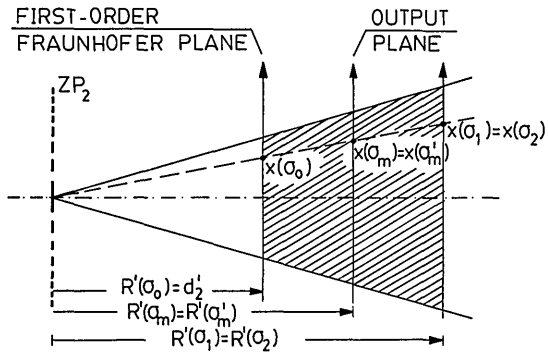

Fig. 5. Same as in Fig. 3 but with $\sigma_0 = \sqrt{\sigma_1\sigma_2}$.

In the same manner, in each transversal plane between d_2' and $R'(\sigma_1)$ we always obtain, with the same scale, the Fraunhofer representation for two different wave numbers.

Because the first-order Fraunhofer plane is always located at one of the ends of the final diffraction volume, with Eq. (24) satisfied it seems more convenient to place the output plane, or achromatic Fraunhofer plane, of the setup at a distance $R'(\sigma_m)$ from ZP_2 (see Fig. 5) such that

$$R'(\sigma_m) = [R'(\sigma_1) + d_2']/2. \tag{25}$$

The scaling of the Fourier transform at this plane, $x(\sigma_m)$, satisfies a similar equation in terms of $x(\sigma_1)$ and $x(\sigma_0)$.

Similarly, we can redefine the chromatic aberration as

$$\begin{aligned} CA_m(\sigma) &= 100[R'(\sigma) - R'(\sigma_m)]/R'(\sigma_m) \\ &= 100[x(\sigma) - x(\sigma_m)]/x(\sigma_m), \end{aligned} \tag{26}$$

which can be written in terms of the previous function $CA_0(\sigma)$ as

$$\begin{aligned} CA_m(\sigma) = [2CA_0(\sigma; \sqrt{\sigma_1\sigma_2}) - CA_0(\sigma_1; \sqrt{\sigma_1\sigma_2})] \\ /[2 + CA_0(\sigma_1; \sqrt{\sigma_1\sigma_2})]. \end{aligned} \tag{27}$$

The zeros of Eq. (27) can be approximately found by solving the equation

$$\sigma/(\sigma - \sigma_0)^2 = 2\sigma_1/(\sigma_1 - \sigma_0)^2, \tag{28}$$

which, using the above-mentioned values for σ_0 and σ_1, has the solutions $\sigma_m = 1.52$ μm^{-1} and $\sigma_m' = 2.29$ μm^{-1}. Hence, from a practical point of view, these solutions are not dependent on the value of α. We also point out that with this choice of the output plane the modulus of the maximum value of both longitudinal and transversal chromatic aberrations is reduced to one half of its primitive value, i.e.,

$$\begin{aligned} |CA_m(\sigma_1)| &= |CA_m(\sigma_2)| = |CA_m(\sqrt{\sigma_1\sigma_2})| \\ &= (1/2)|CA_0(\sigma_1; \sqrt{\sigma_1\sigma_2})|. \end{aligned} \tag{29}$$

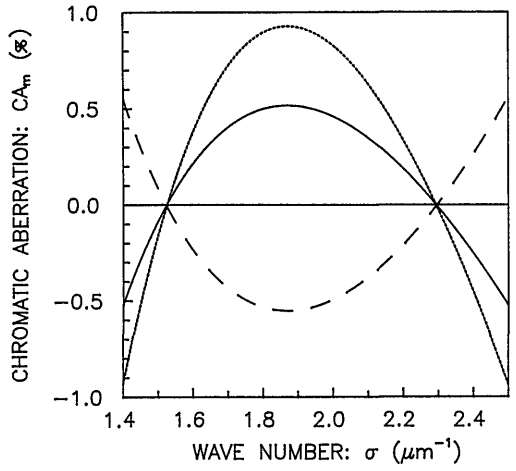

Fig. 6. Plot of the residual chromatic aberration of the optical Fourier transformer in Fig. 2. Short-dashed curve: $f = 150$ mm, $d_2' = 50$ mm, and $Z_0 = -100$ mm (i.e., $\alpha = -4.5$ and $D = 600$ mm); dashed curve: $f = 150$ mm, $d_2' = 45$ mm, and $Z_0 = 65$ mm (i.e., $\alpha = 7.7$ and $D = 975$ mm); solid curve: $f = 180$ mm, $d_2' = 50$ mm, and $Z_0 = -80$ mm (i.e., $\alpha = -8.1$ and $D = 898$ mm).

In Fig. 6 CA_m versus σ is plotted for three different sets of typical values of f, d_2', and Z_0, which determine the value of α and the total length D of the optical arrangement:

$$D = l + f + d_2' = 2Z_0 + 2f + d_2' + (f^2/d_2'). \quad (30)$$

The modulus of the chromatic aberration is less than 1% over the entire visible spectrum in the three cases. Besides, the resulting total length D seems to be adequate for the optical implementation of these cases.

6. Conclusions

In order to achromatize the optical Fourier transforming process, we need to overcome the ordinary behavior of conventional optical systems. For this purpose, we propose a suitable combination of two on-axis, blazed holographic elements and an achromatic lens as an optical Fourier transformer. Our proposal is not completely free from chromatic aberration. So the variations of axial position and scale of the Fourier transform with wave number are found. We point out that such a device provides provides the Fraunhofer diffraction pattern of any pupil, illuminated with a white-light parallel beam, independently of the spectral content of the source and with low residual chromatic aberrations over the entire visible spectrum.

The achromatic Fourier transformer we propose can be considered as a first step in the design of a white-light optical processor.

This research was supported by the Dirección General de Investigación Científica y Técnica (grant PB87-0617), Ministerio de Educación y Ciencia, Spain. W. D. Furlan gratefully acknowledges the financial support of this institution.

References

1. H. Bartelt, S. K. Case, and R. Hauck, "Incoherent optical processing," in *Applications of Optical Fourier Transforms*, H. Stark, ed. (Academic, New York, 1982).
2. W. T. Rhodes and A. A. Sawchuk, "Incoherent optical processing," in *Optical Information Processing*, S. H. Lee, ed. (Springer-Verlag, Berlin, 1981).
3. G. M. Morris and D. A. Zweig, "White-light Fourier transformations," in *Optical Signal Processing*, J. L. Horner, ed. (Academic, New York, 1987).
4. C. Brophy, "Design of an all-glass achromatic Fourier transform lens," Opt. Commun. **47,** 364–368 (1983).
5. G. M. Morris, "An ideal achromatic Fourier processor," Opt. Commun. **39,** 143–147 (1981).
6. G. M. Morris, "Diffraction theory for an achromatic Fourier transformation," Appl. Opt. **20,** 2017–2025 (1981).
7. R. Ferriere and J. P. Goedgebuer, "A spatially coherent achromatic Fourier transformer," Opt. Commun. **42,** 223–225 (1982).
8. R. Ferriere and J. P. Goedgebuer, "Achromatic systems for far-field diffraction with broadband illumination," Appl. Opt. **22,** 1540–1545 (1983).
9. S. Leon and E. N. Leith, "Optical processing and holography with polychromatic point source illumination," Appl. Opt. **24,** 3638–3642 (1985).
10. R. H. Katyl, "Compensating optical systems. Part 3: achromatic Fourier transformation," Appl. Opt. **11,** 1255–1260 (1972).